Article

pubs.acs.org/Biomac

Single-Chain Polymeric Nanocarriers: A Platform for Determining Structure–Function Correlations in the Delivery of Molecular Cargo

Doreen Chan,[†] Anthony C. Yu,[‡] and Eric A. Appel*[,‡]

[†]Department of Chemistry and [‡]Department of Materials Science and Engineering, Stanford University, Stanford, California 94305, United States

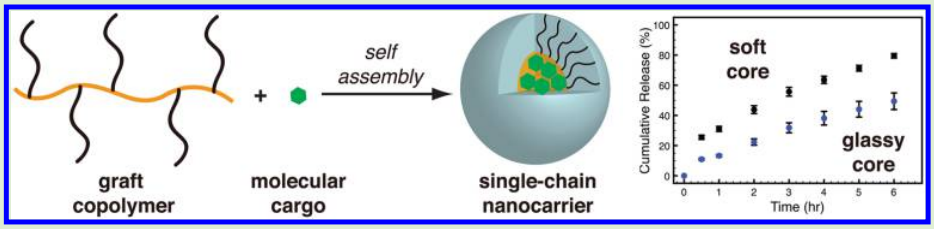

ABSTRACT: There has been growing interest in producing stable, biocompatible nanocarriers for the controlled delivery of therapeutics. With micelles, it remains a challenge to predict a priori the size, aggregation number, and functionality of the self-assembled aggregates. Utilizing controlled radical polymerization techniques, we have prepared tunable high molecular weight amphiphilic comb copolymers that self-assemble into unimolecular "micelle-like" nanocarriers of predictable size and functionality. Excellent control over self-assembly behavior and structure allows for systematic determination of the role of important polymeric material properties (i.e., glass transition) on the release of model therapeutics while simultaneously controlling for size, dispersity, structural, and functionality effects. Moreover, these single-chain polymeric nanocarriers represent a class of drug delivery systems allowing for interrogation of the limitations of standard methods for characterization of micellar aggregates.

INTRODUCTION

A pharmaceutical's therapeutic efficacy is directly related to the manner in which it is administered or delivered to the tissue of interest.[1] Novel delivery technologies, especially nanomaterials, can affect drug pharmacokinetics, absorption, distribution, metabolism, duration of therapeutic effect, excretion, and toxicity, making them highly promising for the management and treatment of disease. Polymeric micelles are a class of nanomaterial of great interest for use as drug carriers, representing a unique hybrid of their natural viral analogs and a synthetic system (Figure 1).[2] Enduring interest in polymer micelles on account of the tunability of their design, their responsiveness to external solutions, high loading efficiency, ability to carry insoluble drugs, and site-specific drug delivery highlights their potential for broad application in pharmaceutical practice.[3]

Despite these advantages, however, the dynamic nature of micelles leads to instabilities in the core and shell, which reduces the degree of control over the incorporation of functional groups and leads to the possibility of complete dissolution at high dilution following systemic injection into the bloodstream.[2,4] Further, it has been well established that the final micelle size has significant effects on the overall behavior of the drug carrier, such as cellular uptake in vivo,[5] transition temperatures,[6] pharmacokinetics,[7] and overall mechanical integrity.[8,9] Notwithstanding the relative ease of making micelles by exploiting the self-assembly behavior of amphiphilic block copolymers, it is challenging to achieve a low size dispersity, and the dynamic nature of these materials compromises nanocarrier stability.[2,10] To overcome these issues, several groups have endeavored to stabilize these micellar aggregates through covalent cross-linking of either the shell or the corona of the micelles following self-assembly.[11−14] This approach, however, has certain limitations on account of the requirement for built-in reactive chemical functionality that may be incompatible with the application of interest.

Alternatively, new nanocarrier architectures have been employed, including star polymers, consisting of a nanogel core with linear arms radiating outward, forming a corona (Figure 1).[15−18] Star polymers have benefited from a unimolecular nature and demonstrated great use in catalysis, emphasizing benefits from single chain character.[19,20] Such single chain unimolecular motifs exploit intramolecular self-assembly that allows for precision and ease of control during particle formation and have been investigated extensively due to their wide range of promising applications and importance.[22,26−30] Thus, they do not suffer from the instabilities associated with traditional micelles, but exhibit similar structural motifs, including a hydrophobic core, hydrophilic corona, and the opportunity for addressable chemical functionality on the periphery. In contrast to conventional micelle formation from block copolymers, processing of many of these unimolecular

Received: February 16, 2017
Published: March 6, 2017

DOI: 10.1021/acs.biomac.7b00249
Biomacromolecules XXXX, XXX, XXX−XXX

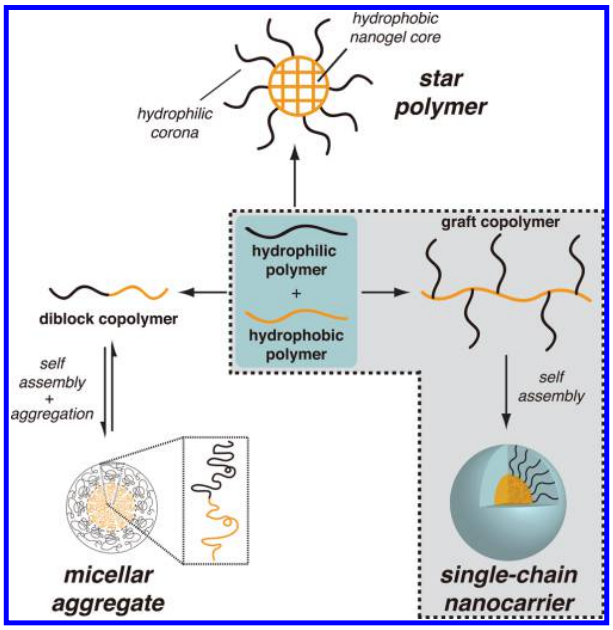

Figure 1. Schematic comparison between polymeric nanocarriers. Amphiphilic block copolymers dynamically self-assemble into micelles exhibiting a critical micelle concentration (CMC). Star polymers (including dendrimers) are high-molecular-weight single molecules exhibiting stable three-dimensional core−shell structures consisting of a "nanogel" core and solvated polymer corona.

shell-cross-linked carriers involves both self-assembly and a subsequent cross-linking step. This secondary cross-linking, in which the hydrophilic side arms shield a collapsed hydrophobic core, inherently alters the chemistry of the corona and greatly affects therapeutic properties, creating the added benefit of stability that controls drug release.[23] These single chain carriers have enhanced properties of stability, robustness against environmental changes, and do not disassemble.[24] While Sawamoto et al. have recently shown the precise control of random copolymers into nanocompartments below a threshold degree of polymerization,[25] the applicability of this molecular architecture has been hindered by the difficulty in specifically obtaining structures of a controlled and desired size, resulting from their poorly controlled syntheses, high dispersity, and low drug-loading capacities on account of their highly chemically cross-linked cores.[18,21]

Here, we precisely tune polymer synthesis to obtain controlled unimolecular three-dimensional micelle-like nanocarriers, involving the intramolecular self-assembly of an amphiphilic graft copolymeric chain, while also monitoring the role of the core glass transition temperature of core-forming polymers on drug release. The formation of these nanocarriers from amphiphilic graft copolymers, driven by intramolecular interactions, is not concentration-dependent, yet still allows for the flexibility and efficiency in cargo loading associated with traditional micellar carriers. We investigate methacrylate derivatives, which exhibit nearly statistical copolymerization under controlled radical polymerization techniques.[31,32] These materials, therefore, provide significant control over the self-assembly process and subsequent polymeric architectures, establishing them as a promising model for determination of materials properties that are key for drug delivery applications.

EXPERIMENTAL SECTION

Instrumentation and Materials. Gel permeation chromatography (GPC) was carried out in tetrahydrofuran (THF) on divinylbenzene columns utilizing a Malvern ViscotekTM TDA 305 triple detection system. Samples were filtered over 0.2 μm PTFE (THF) filters before injection using a 1.0 mL/min flow rate. Molecular weights and polydispersities were determined by comparing to PS standards. Light scattering measurements to determine weight-averaged molecular weight (M_w) were performed with a Wyatt DynaPro NanoStar instrument and the data was analyzed with Wyatt Astra software. The aggregation number (N_A) was determined from the quotient of the micelle M_w and the diblock copolymer M_w. Differential scanning calorimetry (DSC) was performed using a PerkinElmer DSC 8000 with autosampler whereby polymer (5 mg) was heated at 10 °C/min from −20 and 200 °C. Fluorescence measurements were performed with an Infinite M1000 plate reader (Tecan Group, Ltd.). Monomethoxy-poly(ethylene glycol)-methacrylate (PEGMA; M_n ~ 1 kDa) was purchased from Aldrich and was purified by flash chromatography over silica gel, followed by azeotropic distillation with toluene. *t*-Butyl methacrylate (tBMA) and *n*-butyl methacrylate (nBMA) were purchased from Aldrich and purified by flash chromatography over basic alumina and stored at −20 °C over activated molecular sieves. Copper(I) chloride was purified by mixing with acetic acid, dried, rinsed twice with ethanol and dried before use. All other materials were purchased from Aldrich and used as received.

General Synthesis of Graft Copolymers. $PEGMA_{1\ kDa}$ (0.50 g, 0.5 mmol) and nBMA (0.30 g, 2.1 mmol) were dissolved in DMF (1.0 mL). Ethyl α-bromoisobutyrate (15.4 mg, 0.078 mmol) was then dissolved in DMF (1.0 mL). $CuBr_2$ (2.8 mg, 0.013 mmol), TPMA (3.6 mg, 0.013 mmol), and AIBN (8.2 mg, 0.05 mmol) were dissolved in DMF (5.0 mL). All solutions were purged with N_2 for 20 min before initiator stock solution (250 μL) and catalyst stock solution (250 μL) were added to the reaction mixture, which was then stirred at 70 °C for 16 h. The reaction mixture was then quenched by cooling, and the copolymer was recovered by precipitation from cold diethyl ether, collected by filtration, and dried under vacuum to yield a white amorphous polymer (0.69 g, 86%). GPC (THF): M_n (PDI) = 33 kDa (1.19).

General Synthesis of Block Copolymers. Monomer poly(ethylene glycol) methyl ether 2-bromoisobutyrate (mPEG-Br) was synthesized from $PEG_{1\ kDa}$ (1 g, 1 mmol) and *N*,*N*-diisopropylethylamine (0.45 g, 3.5 mmol) stirred in anhydrous DCM (15 mL) in an ice bath. Bromoisobutryl was added dropwise (0.805 g, 3.5 mmol) and stirred overnight. The solution was rotovaped, and unreacted PEG−OH was precipitated out of solution in cold diethyl ether three times. Basic alumina was added to the undissolved solution and solution cooled to collect mPEG-Br and dried overnight. To synthesize the block copolymer, PEG-Br (0.163 g, 0.14 mmol) and nBMA (0.163 g, 1.15 mmol) were added to purged acetone (163 μL). This initiator stock solution was added to a purged solution of copper(I) chloride (6.73 mg, 0.068 mmol) and PMDETA (11.8 mg, 0.068 mmol) in acetone (326 uL) and stirred at 50 °C for 5 h. The reaction mixture was dropped in cold diethyl ether and cooled in the fridge for 30 min to precipitate out block copolymer. The polymer was collected and dried overnight under vacuum.

Preparation of Single-Chain Nanocarriers and Micelles. Single-chain nanocarriers and block copolymer micelles were prepared by dissolving copolymer (5 mg) in acetone (1 mL) and slowly adding DI water (10 mL). The solution was then dialyzed against 1000 mL of DI water for 48 h using a dialysis bag with molecular weight cutoff of 500 Da. The resulting particle-containing solutions were stored at 4 °C until further use.

Measurement of CMC Using Nile Red and Pyrene as a Fluorescent Probe. Aliquots of Nile Red or pyrene in acetone solution (50 μM, 10 μL) were added to containers, which were left in air to evaporate acetone. Aqueous solutions of polymer (1 mL) at varying concentrations were added into the Nile Red containers and left to equilibrate for 24 h. The final dye concentration in each sample is 0.50 μM. For Nile Red, the emission at 590 nm was recorded at an

DOI: 10.1021/acs.biomac.7b00249
Biomacromolecules XXXX, XXX, XXX−XXX

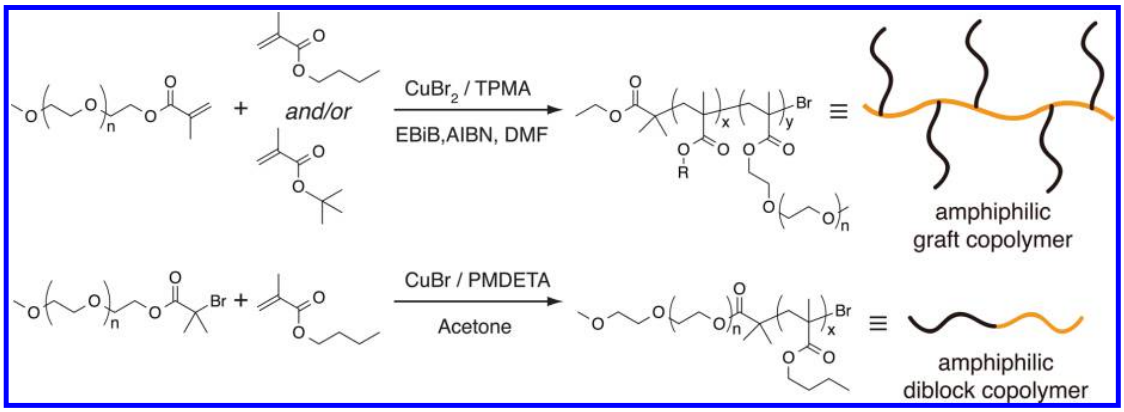

Figure 2. Utilizing Initiators for Continuous Activator Regeneration (ICAR) ATRP with copper(II)bromide ($CuBr_2$), tris(2-pyridylmethyl)amine (TPMA), ethyl α-bromoisobutyrate (EBiB), and 2,2′-Azobis(2-methylpropionitrile) (AIBN), *n*-butyl methacrylate (*n*BMA; low T_g) and/or *tert*-butyl methacrylate (*t*BMA; high T_g), and poly(ethylene glycol)methacrylate ($M_n \sim 1$ kDa) were polymerized to produce amphiphilic graft copolymers (P(*x*BMA-*g*-PEG)) with exquisite control over molecular weight, polydispersity, and the number of polymeric grafts (N_G). Additionally, traditional amphiphilic block copolymers (PEG-*b*-PnBMA) were prepared for comparison.

excitation wavelength of 525 nm. Both the excitation and emission bandwidths were set at 2.5 nm. For pyrene, the emission ratio of 372−383 nm was recorded at an excitation wavelength of 334 nm. In both experiments, the emission intensity (peak height) was analyzed as a function of polymer concentration and the CMC was taken from the inflection point.

Characterization of Model Drug Release. Micelles or single-chain nanocarriers were prepared as described above, yet with fluorescein (0.1 mg, 2% relative to polymer) codissolved in acetone with the copolymer species. The solution was transferred into a dialysis bag with a molecular weight cutoff of 500 Da. The bag was then immersed into a container with 50 mL of PBS at 37 °C. At specific time intervals, the entire medium was removed and replaced with fresh buffer. The sample medium was analyzed using fluorescence spectroscopy and the cumulative release over time determined. The experiment was repeated in triplicate.

RESULTS AND DISCUSSION

Recent years have seen the development of specialized radical polymerization techniques, especially those based on atom transfer radical polymerization (ATRP), that afford access to high molecular weight polymeric materials. Indeed, amphiphilic comb copolymers have been prepared with excellent control over molecular weight, dispersity ($Đ$), and number of polymeric grafts (N_G).[33] Utilizing Initiators for Continuous Activator Regeneration (ICAR) ATRP with copper(II)bromide ($CuBr_2$), tris(2-pyridylmethyl)amine (TPMA), ethyl α-bromoisobutyrate (EBiB), and 2,2′-Azobis(2-methylpropionitrile) (AIBN),[34] we prepared amphiphilic comb copolymers from *n*-butyl methacrylate (nBMA), a low T_g polymer, or *t*-butyl methacrylate (tBMA), a high T_g polymer, and poly(ethylene glycol)methacrylate to produce amphiphilic graft copolymers, P(*x*BMA-*g*-PEG) (Figure 2; Table 1). By simply altering the formulation of nBMA and tBMA in the graft copolymers, it was possible to tune the glass transition of the resulting copolymer backbones, allowing for the formation of micellar materials with similar chemical properties (e.g., relative hydrophobicity) and physical structures (e.g., size and N_G), yet with differing physical properties (e.g., soft or glassy hydrophobic cores).

With graft copolymers in hand, self-assembled micelle-like materials were formed, containing varying amounts of nBMA and tBMA and were compared with micellar aggregates formed from analogous amphiphilic block copolymers, PEG-*b*-PnBMA

Table 1. Characterization of Amphiphilic Copolymers Used in This Study

entry[a]	nBMA/tBMA (w/w)	T_g[b] (°C)	M_n[c] (kDa)	$Đ$[d]	N_G[e]	size[d] (nm)
1	100:0	20	33	1.19	20	8.7
2	90:10	28	35	1.20	21	9.6
3	70:30	44	31	1.21	19	9.0
4	0:100	118	34	1.18	21	10.1
5	100:0	20	1.6	1.11	19[f]	10.9

[a]Prepared with PEGMA ($M_n \sim 1$ kDa) and thus comprising 62.5% (w/w) PEG relative to total *x*BMA content. [b]DSC analysis. [c]THF GPC analysis. [d]Light scattering analysis in water. [e]Graft density, N_G, determined for single-chain nanocarriers. [f]Aggregation number, N_A, determined for micellar aggregates.

(Table 1). Light scattering measurements were performed to characterize the size and absolute weight-averaged molecular weight (M_w) of the micellar materials to differentiate single-chain nanocarriers from comparable amphiphilic diblock copolymer micelles. When PEG-*b*-PnBMA diblock copolymer was dissolved in DMF, which completely dissolves the polymer, thus precluding the formation of micelles, the polymer exhibited M_w = 1.9 kDa (Figure 3a). In contrast, when this polymer was formulated in water, micellar aggregates were formed, which exhibited M_w = 35 kDa (Figure 3a), corresponding to an aggregation number, N_A, of 19 block copolymers per micelle. Yet, when the same conditions were imposed on the P(nBMA-*g*-PEG)-based materials, a single overlapping peak was observed, whereby M_w = 39 kDa in DMF and 45 kDa in water, thus, illustrating that the nanocarriers comprise a single polymer chain (Figure 3b). In these materials, the graft density, N_G (comparable to the aggregation number, N_A, of standard diblock copolymer micelles), is predetermined by the formulation of the polymerization, providing exquisite control over the functionality of the resulting architectures.

We then investigated the ability of these single-chain nanocarriers to form self-assembled molecular occlusion complexes using model molecular cargo. Slow addition of water to a solution of the amphiphilic graft copolymer and Nile Red from a water-miscible organic solvent capable of completely dissolving both the polymer and the dye (e.g., acetone) formed a clear, colored, aqueous solution, whereas

DOI: 10.1021/acs.biomac.7b00249
Biomacromolecules XXXX, XXX, XXX−XXX

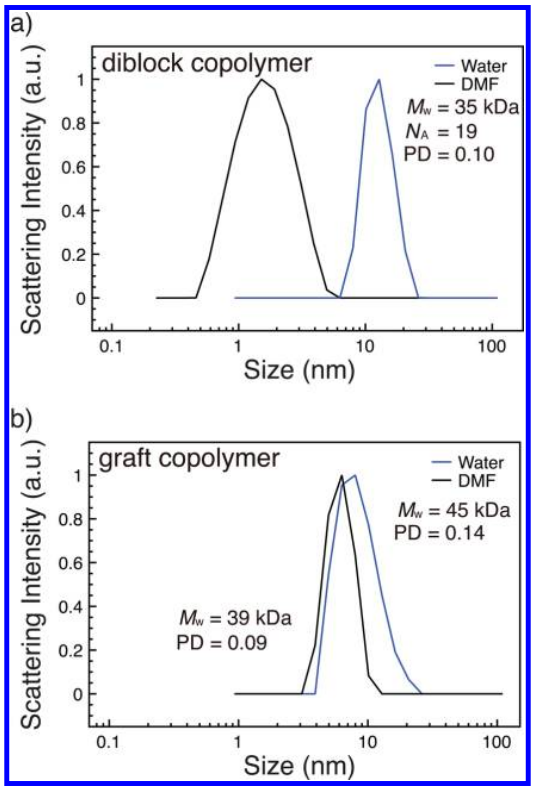

Figure 3. Light scattering characterization of (a) PEG-*b*-PnBMA and (b) P(nBMA-*g*-PEG) in DMF (which completely solvates the polymer) and water (selectively solvates the PEG grafts, leading to self-assembly). Size and absolute weight-averaged molecular weight (M_w) of the polymers in these solvents demonstrate that P(nBMA-*g*-PEG) polymers form nanomaterials composed of a single polymer chain, which is clearly differentiated from analogous amphiphilic diblock copolymer micelles.

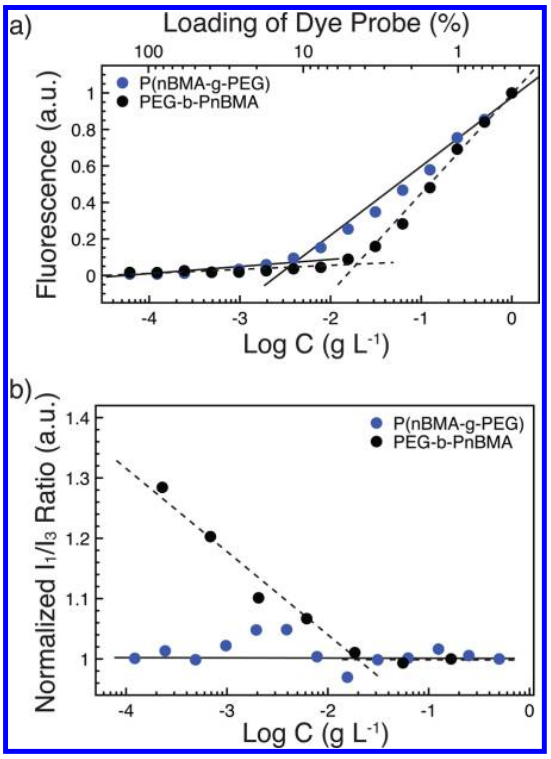

Figure 4. (a) Normalized fluorescence intensity of encapsulated Nile Red dye probe plotted against the concentration of polymeric species and against the relative loading of dye probe within the nanocarrier. Utilization of dye encapsulation to characterize the CMC (or lack thereof) in these diblock copolymer micelles and single-chain nanocarriers is inherently limited in scope as low polymer concentrations equate to exceptionally high dye loading. (b) Normalized ratio of the fluorescence intensity of I_1 to I_3 from encapsulated pyrene plotted against the concentration of polymeric species yields a CMC for diblock copolymer micelles and none observed for single-chain nanocarriers.

introduction of water to a solution of the dye alone induced precipitation of the dye. To demonstrate the lack of concentration dependence for single-chain nanocarrier formation, the critical micelle concentration (CMC) for these materials was characterized using Nile Red encapsulation (Figure 4a). For micelles formed from PEG-*b*-PnBMA diblock copolymers, we determined a CMC of 19.5 mg/mL, which is similar to values reported for many other reported diblock copolymer micelle systems.[35] Surprisingly, we also observe a CMC-like transition in the case of P(nBMA-*g*-PEG) single-chain nanocarrier at 3.58 mg/mL, which is not expected to show concentration-dependent formation on account of its intramolecular self-assembly process. It is possible to rationalize these observations, however, when one considers the relative loading of dye probe within the micelle/nanocarrier, which is inherently limited by the solubility of the dye probe in the core of micelles. In the case of PEG-*b*-PnBMA diblock copolymer micelles, the ultimate loading of Nile Red at the observed CMC is 3.2% (w/w), which is well within a reasonable loading of molecular cargo within such micellar aggregates.[36] However, in the case of P(nBMA-*g*-PEG) single-chain nanocarriers, the ultimate loading of dye probe at the observed "CMC" is 10.5%, which is similar to the expected maximal loading for any carrier of this nature.[36] Therefore, below a certain concentration of polymeric species, insufficient dye probe enters the "micelle-like" structure to be observed, regardless of whether or not structures are present.

These observations highlight that typical dye encapsulation methods for CMC-determination of micelle formation from amphiphilic copolymers must have a lower threshold of observable CMCs, determined by the maximum loading of the dye probe within the polymer aggregate, and demonstrate the need for innovative new techniques for micelle characterization.

To more accurately characterize the concentration dependence of our single-chain nanocarriers, we redesigned the dye probe assay. We prepared aqueous solutions of pyrene-loaded single-chain nanocarriers and comparable diblock copolymer micelles comprising concentrations of polymer (0.5 g/L) and pyrene (50 μM) corresponding to 1% (w/w) loading of dye probe within the nanocarriers. These solutions were then serially diluted with water and the fluorescence intensity at I_1 = 372 nm and I_3 = 383 nm was measured. The ratio of these values (I_1/I_3) has been broadly used to characterize micelle CMC values, as this ratio can indicate the pyrene's local environment, such as when loaded into micelles.[37] Here, by monitoring a change in the ratio of fluorescence intensity as a function of nanocarrier concentration, we can characterize the stability of the carrier during dilution, as the change will

DOI: 10.1021/acs.biomac.7b00249
Biomacromolecules XXXX, XXX, XXX−XXX

correspond to the CMC. This assay yielded a CMC value of 15.1 mg/mL for PEG-*b*-PnBMA diblock copolymer micelles, consistent with our previous observations, while no transition was observed for the P(nBMA-*g*-PEG) single-chain nanocarriers (Figure 4b). These data are consistent with the expected self-assembly behavior for these materials.

We then exploited these materials to elucidate the effect of specific materials properties such as the glass transition temperature (T_g) of the core-forming polymer backbone, in determining the release characteristics of molecular cargo (fluorescein) at physiologic temperatures. The molecular cargo was again encapsulated into the nanocarriers by cointroduction of the cargo and copolymer into water. Once encapsulated, the release characteristics of the cargo from nanocarriers comprising low T_g graft copolymers were compared to those comprising high T_g copolymers. Solvent self-diffusion models describe transport behavior of a solute in polymer−solvent systems to be strongly dependent on the specific free volume, and thus the mobility, of the mixture. Accordingly, a polymer in a glassy state is expected to exhibit slower solute diffusion on account of a lower specific free volume.[38] Indeed, release of the model cargo from single-chain nanocarriers containing a high T_g hydrophobic polymer core shows significantly more sustained release when compared with the release from single-chain nanocarriers containing a low T_g hydrophobic polymer core (Figure 5a), presumably on account of the slower diffusion through the glassy polymer.[39,40] Using the Ritger-Peppas equation, we extracted values for the diffusional release rate, *k*, and release order, *n*, of the model cargo from the graft copolymer nanocarriers (Figure 5b).[41,42] The release rates follow an interesting trend, whereby $k \sim 15\%/h$ for both polymers that are glassy under physiologic conditions (i.e., $T_g > 37$ °C), while $k \sim 30\%/h$ for both polymers that are soft under physiologic conditions (i.e., $T_g < 37$ °C). The release rates, therefore, for cargo from glassy materials is significantly slower than for the soft materials. Moreover, the values of *n* follow a similar trend, whereby both soft polymers exhibit Fickian diffusional cargo release ($n \sim 0.45 - 0.5$), while both glassy polymers exhibit a combination of Fickian and anomalous diffusional release ($n \sim 0.65$). These observations highlight that the enhanced molecular mobility above the T_g of the core polymers allows for facile diffusion of cargo. In contrast, below the T_g of the core polymers, when they are glassy, diffusion of molecular cargo is significantly hindered and thus requires an anomalous combination of cargo diffusion and polymer chain mobility for release to occur. On account of the highly controlled nature of the carriers used in this studies, whereby size, aggregation number, hydrophobicity, drug encapsulation, and chemical functionality were all controlled for, we highlight that the core polymer T_g can indeed be exploited as an important design parameter for optimization of molecular cargo release micellar nanocarriers.

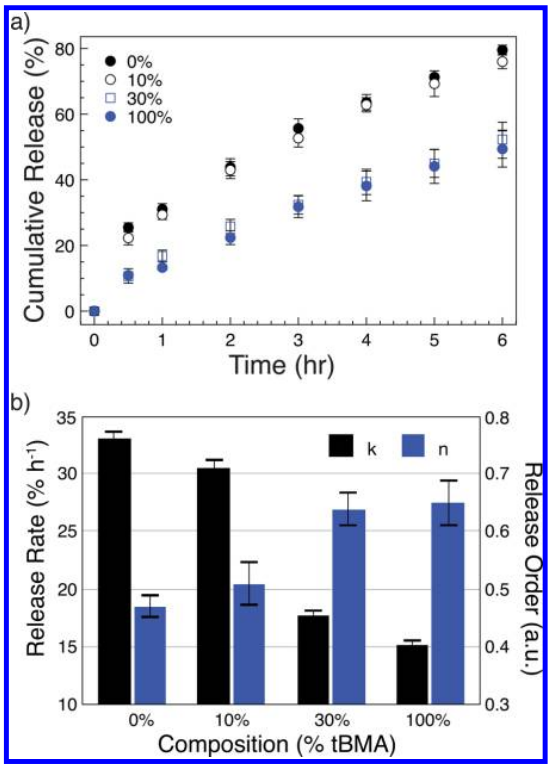

Figure 5. Encapsulation and release of a model drug compound (fluorescein) demonstrates that single-chain nanocarriers containing a high T_g polymer core lead to more sustained release ($k \sim 15\%/h$) when compared with a low T_g hydrophobic polymer core ($k \sim 30\%/h$) as diffusion of the dye is both slower and anomalous in nature in a glassy polymer. (a) Cumulative release plot and (b) corresponding quantification of release characteristics.

CONCLUSIONS

In summary, an efficient, highly controlled synthesis of complex polymer architectures has been accessed with innovative CRP techniques. Control over their size and endowment of functionality to these materials, both in the core and about their periphery, is facile through modulation of the polymerization formulation. Intramolecular self-assembly leads to robust hydrophilic/hydrophobic core−shell nanocarriers composed of a single polymer chain and capable of forming reversible occlusion complexes with hydrophobic molecules, which may include pharmaceuticals. These materials allow for the systematic determination of the role of important polymeric material properties (i.e., glass transition temperature and relative hydrophobicity) on the loading and release behavior of model therapeutics while controlling for size, structural, and functionality effects. In future studies, incorporation of stimuli-responsive functionality into the hydrophobic backbone (e.g., incorporation of pH, temperature or chemically responsive monomers) of the graft copolymers can potentially afford external control over the self-assembly process for these particles, thus, providing a mechanism for stimuli-responsive release of molecular cargo from these single-chain nanocarriers. These unimolecular carriers offer possibilities with further functionalities and possibilities. The fundamental knowledge from this study will hopefully facilitate progress in the field of drug delivery, providing prescriptive models for the development of more effective nanocarriers.

AUTHOR INFORMATION

Corresponding Author

*E-mail: eappel@stanford.edu.

ORCID

Eric A. Appel: 0000-0002-2301-7126

DOI: 10.1021/acs.biomac.7b00249
Biomacromolecules XXXX, XXX, XXX−XXX

Author Contributions

The manuscript was written through contributions of all authors. All authors have given approval to the final version of the manuscript.

Notes

The authors declare no competing financial interest.

■ ACKNOWLEDGMENTS

D.C. is grateful for an award by the Department of Defense, Air Force Office of Scientific Research, National Defense Science and Engineering Graduate (ND-SEG) Fellowship, 32 CFR 168a with government support under FA9550-11-C-0028. E.A.A. is extremely grateful for a Frederick E. Terman Faculty Fellowship and a Hellman Faculty Fellowship.

■ REFERENCES

(1) Tibbitt, M.; Dahlman, J.; Langer, R. *J. Am. Chem. Soc.* **2016**, *138*, 704−717.
(2) O'Reilly, R. K.; Hawker, C. J.; Wooley, K. L. *Chem. Soc. Rev.* **2006**, *35*, 1068−1083.
(3) Gao, Z.; Lukyanov, A. N.; Singhai, A.; Torchilin, V. P. *Nano Lett.* **2002**, *2*, 979−982.
(4) Shenhar, R.; Norsten, T. B.; Rotello, V. M. *Adv. Mater.* **2005**, *17*, 657−669.
(5) He, C.; Hu, Y.; Yin, L.; Tang, C.; Yin, C. *Biomaterials* **2010**, *31*, 3657−3666.
(6) Leong, N. S.; Brebis, K.; E, D. L.; O'Reilly, R. K.; Gibson, M. I. *Chem. Commun.* **2011**, *47*, 11627−11629.
(7) Minchin, R. *Nat. Nanotechnol.* **2008**, *3*, 12−13.
(8) Balazs, A. C.; Emerick, T.; Russell, T. P. *Science* **2006**, *314*, 1107−1110.
(9) Jiang, W.; Kim, B. Y. S.; Rutka, J. T.; Chan, W. C. W. *Nat. Nanotechnol.* **2008**, *3*, 145−150.
(10) Karnik, R.; Gu, F.; Basto, P.; Cannizzaro, C.; Dean, L.; Kyei-Manu, W.; Langer, R.; Farokhzad, O. *Nano Lett.* **2008**, *8*, 2906−2912.
(11) Wooley, K. L.; Hawker, C. J.; Frechet, J. M. J. *J. Am. Chem. Soc.* **1991**, *113*, 4252−4261.
(12) Kim, Y.; Pourgholami, M. H.; Morris, D. L.; Lu, H.; Stenzel, M. H. *Biomater. Sci.* **2013**, *1*, 265−275.
(13) Read, E. S.; Armes, S. P. *Chem. Commun.* **2007**, 3021−3035.
(14) Kim, Y.; Liemmawal, E. D.; Pourgholami, M. H.; Morris, D. L.; Stenzel, M. H. *Macromolecules* **2012**, *45*, 5451−5462.
(15) Hawker, C. J.; Frechet, J. M. J.; Grubbs, R. B.; Dao, J. *J. Am. Chem. Soc.* **1995**, *117*, 10763−10764.
(16) Miller, R. D.; Yusoff, R. M.; Swope, W. C.; Rice, J. E.; Carr, A. C.; Parker, A. J.; Sly, J.; Appel, E. A.; Nguyen, T.; Piunova, V. *Polymer* **2015**, *79*, 255−261.
(17) Appel, E. A.; Lee, V. Y.; Nguyen, T.; McNeil, M.; Nederberg, F.; Hedrick, J. L.; Swope, W. C.; Rice, J. E.; Miller, R. D.; Sly, J. *Chem. Commun.* **2012**, *48*, 6163−6165.
(18) Lee, V. Y.; Havenstrite, K.; Tjio, M.; McNeil, M.; Blau, H. M.; Miller, R. D.; Sly, J. *Adv. Mater.* **2011**, *23*, 4509−4515.
(19) Terashima, T.; Kamigaito, M.; Baek, K.; Ando, T.; Sawamoto, M. *J. Am. Chem. Soc.* **2003**, *125*, 5288−5289.
(20) Kanaoka, S.; Yagi, N.; Fukuyama, Y.; Aoshima, S.; Tsunoyama, H.; Tsukuda, T.; Sakurai, H. *J. Am. Chem. Soc.* **2007**, *129*, 12060−12061.
(21) Liu, M.; Kono, K.; Frechet, J. M. J. *J. Controlled Release* **2000**, *65*, 121−131.
(22) Gonzalez-Burgos, M.; Latorre-Sanchez, A.; Pomposo, J. A. *Chem. Soc. Rev.* **2015**, *44*, 6122−6142.
(23) Sosnik, A.; Raskin, M. M. *Biotechnol. Adv.* **2015**, *33*, 1380−1392.
(24) Williams, R. J.; Pitto-Barry, A.; Kirby, N.; Dove, A. P.; O'Reilly, R. K. *Macromolecules* **2016**, *49*, 2802−2813.
(25) Hirai, Y.; Terashima, T.; Takenaka, M.; Sawamoto, M. *Macromolecules* **2016**, *49*, 5084−5091.
(26) Harth, E.; Van Horn, B.; Lee, V. Y.; Germack, D. S.; Gonzales, C. P.; Miller, R. D.; Hawker, C. J. *J. Am. Chem. Soc.* **2002**, *124*, 8653−8660.
(27) Mecerreyes, D.; Lee, V.; Hawker, C.; Hedrick, J. L.; Wursch, A.; Volksen, W.; Magbitang, T.; Huang, E.; Miller, R. D. *Adv. Mater.* **2001**, *13*, 204−208.
(28) Appel, E. A.; Dyson, J.; del Barrio, J.; Walsh, Z.; Scherman, O. A. *Angew. Chem., Int. Ed.* **2012**, *51*, 4185−4189.
(29) Appel, E. A.; del Barrio, J.; Dyson, J.; Isaacs, L.; Scherman, O. A. *Chem. Sci.* **2012**, *3*, 2278−2281.
(30) Shokeen, M.; Pressly, E. D.; Hagooly, A.; A, Z.; Ramos, N.; Fiamengo, A. L.; Welch, M. J.; Hawker, C. J.; Anderson, C. J. *ACS Nano* **2011**, *5*, 738−747.
(31) Haddleton, D. M.; Crossman, M. C.; Hunt, K. H.; Topping, C.; Waterson, C.; Suddaby, K. G. *Macromolecules* **1997**, *30*, 3992−3998.
(32) Brar, A. S.; Kapur, G. S. *Polym. J.* **1988**, *20*, 811−817.
(33) Matyjaszewski, K.; Tsarevsky, N. V. *Nat. Chem.* **2009**, *1*, 276−288.
(34) Matyjaszewski, K.; Jakubowski, W.; Min, K.; Tang, W.; Huang, J.; Braunecker, W. A.; Tsarevsky, N. V. *Proc. Natl. Acad. Sci. U. S. A.* **2006**, *103*, 15309−15314.
(35) Nederberg, F.; Appel, E. A.; Tan, J. P. K.; Kim, S. H.; Fukushima, K.; Sly, J.; Miller, R. D.; Waymouth, R. M.; Yang, Y. Y.; Hedrick, J. L. *Biomacromolecules* **2009**, *10*, 1460−1468.
(36) Ke, X.; Ng, V. W. L.; Ono, R. J.; Chan, J. M. W.; Krishnamurthy, S.; Wang, Y.; Hedrick, J. L.; Yang, Y. Y. *J. Controlled Release* **2014**, *193*, 9−26.
(37) Ananthapadmanabhan, K. P.; Goddard, E. D.; Turro, N. J.; Kuo, P. L. *Langmuir* **1985**, *1*, 352−355.
(38) Vrentas, J. S.; Vrentas, C. M. *Macromolecules* **1994**, *27*, 5570−5576.
(39) Ritger, P.; Peppas, N. *J. Controlled Release* **1987**, *5*, 23−36.
(40) Ritger, P.; Peppas, N. *J. Controlled Release* **1987**, *5*, 37−42.
(41) Choi, S. H.; Park, T. G. *J. Biomater. Sci., Polym. Ed.* **2002**, *13*, 1163−1173.
(42) Siepmann, J.; Peppas, N. *Adv. Drug Delivery Rev.* **2012**, *64*, 163−174.

DOI: 10.1021/acs.biomac.7b00249
Biomacromolecules XXXX, XXX, XXX−XXX